

Infrared polarimetry and photometry of BL Lac objects – II

C. D. Impey *Institute for Astronomy, University of Hawaii,
2680 Woodlawn Drive, Honolulu, Hawaii 96822, USA*

P. W. J. L. Brand *Department of Astronomy, University of Edinburgh,
Blackford Hill, Edinburgh EH9 3HJ, Scotland*

R. D. Wolstencroft *Royal Observatory Edinburgh, Blackford Hill,
Edinburgh EH9 3HJ, Scotland*

P. M. Williams *United Kingdom Infrared Telescope Unit, 900 Leilani Street,
Hilo, Hawaii 96720, USA*

Received 1983 November 15; in original form 1982 April 14

Summary. Photometry and polarimetry in the *JHK* wavebands have now been obtained for 25 BL Lac objects, more than doubling the amount of data contained in Paper I (Impey *et al.* 1982a). Several new objects have been monitored for periods of up to five days, and accumulated data is sufficient for a statistical analysis of polarization properties. The selection effects operating on this sample are examined first. A power-law spectrum is consistent with the spectra of all but three objects. Important new results are (1) The four most luminous sources show indirect evidence for relativistic bulk motion of the emitting volume; (2) The range of position angles from monitoring correlates well with infrared luminosity; (3) The maximum $2.2\ \mu\text{m}$ polarization and maximum $1\text{--}2\ \mu\text{m}$ spectral index are correlated; (4) The sample divides into two distinct parts: one where the change in total and polarized flux are closely correlated, and the other where they are not correlated at all; (5) Strong wavelength-dependent polarization is observed in only two out of thirteen objects; (6) The amplitude of polarization variations between day and month time-scales is constant, while the amplitude of flux variations increases; (7) There is good evidence that transitions in polarization and position angle are ‘decoupled’; i.e., changes in position angle take place at a constant degree of polarization.

1 Introduction

This paper presents results from a continuing program to monitor the infrared polarization of BL Lac objects. Data from the first year of monitoring has previously been published

(Impey *et al.* 1982a, Paper I). Infrared polarimetry and photometry have now been obtained for 19 BL Lac objects, with photometry alone for another six. The data contained here doubles the amount of polarimetry in Paper I, and adds a considerable amount of new photometry. Where possible, polarization measurements have been made in more than one colour. The sample now represents a considerable fraction of the number of known BL Lac objects (Angel & Stockman 1980; Weiler & Johnston 1980). As expected, the infrared continua of many BL Lac objects are dominated by strongly variable flux and polarization. However, a sufficient database has now been established to examine the polarization properties of BL Lac objects statistically.

2 Observations

The observations were all carried out at the 3.8-m United Kingdom Infrared Telescope (UKIRT) on Mauna Kea using a photovoltaic InSb detector and rotating HR Polaroid. All the polarization data were collected in two separate runs during the period 1981 April/May. The photometry was collected over the period 1980 April to 1981 May. The two runs in 1981 April/May used the $f/35$ chopping secondary with star/sky chopping at a rate of 7–8 Hz. The instrumental parameters were re-determined for each run and the instrumental sensitivity and polarization were calculated an average of twice a night. The broad band filters used and their effective wavelengths were: $J(1.25 \mu\text{m})$, $H(1.65 \mu\text{m})$ and $K(2.2 \mu\text{m})$.

The calibration and reduction procedures for this project were described in Paper I, the same procedures have been followed for the data presented here. The analyzer efficiency and position angle zero point were re-determined each time the polarimeter was mounted on the telescope. The polarimetry was calibrated with nearby unpolarized stars, and the instrumental polarization was repeatable over a run to an rms of 0.3 per cent. Fluxes in absolute units have been corrected for the effect of the different flux distributions of the objects and the calibrators in the broad passbands. Repeated measurements of standard stars showed that the instrumental magnitudes during the two runs in 1981 April/May had rms deviations of no more than 1.8 per cent and 2.4 per cent. For faint BL Lac objects where polarimetry was not possible, the analyzer was removed from the light path to enable faster photometry to be carried out. Nine observations were made with the analyzer both in and out. Due to uncertainties in the primary calibrators, the zero point of the absolute flux scale is only accurate to about 5 per cent.

The BL Lac objects were acquired either directly on the integrating Quantex TV system or indirectly by offsetting from a nearby bright star with accurate coordinates. The offsetting was in general accurate to ± 0.5 arcsec, and in all cases was checked by peaking up on the $2.2 \mu\text{m}$ signal of the object. The beam positions were checked on each new object, and also whenever the telescope passed through the meridian. All the observations in 1981 April/May were made using a 10 arcsec aperture, and since all of the BL Lac objects were stellar, no aperture corrections were needed. Flat-topped beam profiles and accurate auto-guiding ensured the integrity of the photometry. All the observations were made in or near dark of Moon.

3 Results

Individual objects are discussed below, with the exception of those whose polarimetric histories were given in Paper I. The results are presented in Table I, where column (1) gives the Parkes designation and any other source name, column (2) gives the date (UT) of the obser-

Table 1. Details of polarimetry and photometry for all the objects.

(1)	(2)	(3)	(4)	(5)	(6)	(7)
Object	Date	Aperture	Waveband	$p \pm \sigma(p)$	$\theta \pm \sigma(\theta)$	$S \pm \sigma(S)$
0735+178 (PKS)	4 Apr 81	10"	K	13.1 ± 3.4	28 ± 7.1	11.6 ± 0.3
			H	15.0 ± 7.6	40 ± 7.6	9.8 ± 0.3
	5 Apr 81	10"	K	14.4 ± 4.6	17 ± 8.7	18.3 ± 0.7
			J	12.7 ± 4.5	170 ± 9.7	9.0 ± 0.7
	6 Apr 81	10"	K	14.0 ± 1.1	10 ± 2.1	16.5 ± 0.5
			H	16.6 ± 3.3	12 ± 5.4	9.2 ± 0.3
			J	20.9 ± 5.0	10 ± 6.5	5.5 ± 0.2
	7 Apr 81	10"	K	10.4 ± 2.6	12 ± 4.7	17.9 ± 0.5
			H	16.4 ± 2.0	12 ± 2.3	11.4 ± 0.2
	8 Apr 81	10"	K	15.4 ± 2.0	167 ± 3.5	18.4 ± 0.6
			H	15.3 ± 2.1	170 ± 2.7	13.7 ± 0.3
	30 Apr 81	10"	K	24.7 ± 1.1	155 ± 1.3	23.9 ± 0.7
			H	22.7 ± 2.7	155 ± 3.2	18.3 ± 0.9
	2 May 81	10"	K	26.4 ± 2.2	163 ± 2.3	28.2 ± 0.8
			H	29.6 ± 2.3	161 ± 2.1	20.4 ± 1.0
			J	32.6 ± 3.0	163 ± 2.5	14.7 ± 0.3
	3 May 81	10"	K	20.8 ± 0.8	163 ± 1.1	23.0 ± 1.2
			H	20.7 ± 1.8	167 ± 2.4	17.2 ± 0.9
J			26.4 ± 3.7	162 ± 3.8	13.3 ± 0.7	
4 May 81	10"	K	22.7 ± 2.4	158 ± 2.9	16.8 ± 0.5	
		H	23.5 ± 3.7	152 ± 4.3	7.3 ± 0.4	
		J	13.3 ± 6.8	168 ± 14	6.2 ± 0.1	
0754+101 (OI 090.4)	4 Apr 81	10"	K	18.9 ± 6.7	112 ± 9.7	10.9 ± 0.3
	5 Apr 81	10"	K	12.9 ± 4.8	109 ± 10	13.6 ± 0.6
	6 Apr 81	10"	K	12.1 ± 6.2	89 ± 13	12.0 ± 0.4
	7 Apr 81	10"	K	4.2 ± 3.4	172 ± 22	16.5 ± 0.5
	8 Apr 81	10"	K	2.7 ± 1.5	102 ± 15	12.0 ± 0.4
0818-128 (OJ-131)	7 Apr 81	10"	K	14.4 ± 2.5	122 ± 4.7	13.9 ± 0.4
			H	17.9 ± 6.1	128 ± 9.3	10.2 ± 0.3
			J	21.4 ± 9.9	126 ± 13	9.4 ± 0.2
	8 Apr 81	10"	K	13.7 ± 3.2	91 ± 6.2	11.9 ± 0.4
	2 May 81	10"	K	8.7 ± 2.1	91 ± 6.6	19.1 ± 0.6
			H	6.0 ± 1.9	104 ± 8.6	15.6 ± 0.8
3 May 81	10"	K	14.0 ± 5.0	128 ± 4.8	16.7 ± 0.8	
0851+202 (OJ 287)	5 Apr 81	10"	K	16.8 ± 3.6	151 ± 5.9	11.7 ± 0.4
	6 Apr 81	10"	K	12.0 ± 2.3	142 ± 5.2	15.2 ± 0.5
			H	15.6 ± 2.5	152 ± 4.4	10.3 ± 0.2
	7 Apr 81	10"	K	12.9 ± 2.4	165 ± 5.1	17.1 ± 0.5
			H	15.9 ± 3.0	150 ± 5.2	10.9 ± 0.2
	8 Apr 81	10"	K	11.9 ± 1.5	133 ± 3.4	14.9 ± 0.4
	2 May 81	10"	K	18.9 ± 4.2	125 ± 3.8	20.6 ± 0.6
			H	19.7 ± 1.9	124 ± 2.6	13.0 ± 0.7
J	15.0 ± 1.4	113 ± 2.5	8.9 ± 0.2			
0912+297 (OK 222)	6 Apr 81	10"	K	12.2 ± 5.0	2.9 ± 11.2	8.0 ± 0.2
	8 Apr 81	10"	K	5.1 ± 4.9	128 ± 26	6.8 ± 0.2

Table 1 – continued

(1)	(2)	(3)	(4)	(5)	(6)	(7)	
Object	Date	Aperture	Waveband	$p \pm \sigma(p)$	$\theta \pm \sigma(\theta)$	$S \pm \sigma(S)$	
1156+295 (4C 29.45)	4 Apr 81	10"	K	11.2 ± 0.7	21.8 ± 1.7	54.2 ± 1.1	
			H	12.5 ± 2.3	21.5 ± 5.0	34.5 ± 0.7	
	5 Apr 81	10"	K	14.3 ± 0.9	31.6 ± 1.7	74.8 ± 1.5	
			J	15.3 ± 1.7	22.3 ± 3.0	47.7 ± 1.4	
	6 Apr 81	10"	K	10.0 ± 1.8	13.0 ± 4.9	40.7 ± 0.8	
			H	10.3 ± 0.9	22.8 ± 2.4	27.2 ± 0.5	
			J	10.4 ± 1.4	18.7 ± 3.7	22.0 ± 0.7	
	7 Apr 81	10"	K	5.5 ± 1.1	0.5 ± 4.0	49.9 ± 1.0	
			H	4.7 ± 2.1	166 ± 12	32.4 ± 0.6	
			J	3.6 ± 2.1	161 ± 16	25.5 ± 0.8	
	8 Apr 81	10"	K	8.9 ± 1.6	158 ± 4.9	32.9 ± 0.7	
			H	11.3 ± 1.1	157 ± 2.7	23.9 ± 0.5	
	30 Apr 81	10"	K	8.3 ± 5.4	54 ± 18	8.7 ± 0.3	
	2 May 81	10"	K	8.3 ± 2.5	108 ± 8.2	12.0 ± 0.4	
3 May 81	10"	K	5.6 ± 0.9	161 ± 4.4	14.4 ± 0.6		
4 May 81	10"	K	11.6 ± 3.0	128 ± 7.1	9.7 ± 0.2		
1253-055 (3C 279)	6 Apr 81	10"	K	16.2 ± 4.1	67.8 ± 6.9	5.1 ± 0.2	
	8 Apr 81	10"	K	9.7 ± 6.2	98.4 ± 17	6.2 ± 0.2	
1308+326 (B2)	3 May 81	10"	K	11.4 ± 3.1	85.8 ± 7.4	9.0 ± 0.9	
	4 May 81	10"	K	20.1 ± 3.3	99.5 ± 4.5	8.1 ± 0.2	
1418+546 (OQ 530)	6 Apr 81	10"	K	17.9 ± 7.8	59.3 ± 12	6.5 ± 0.4	
	2 May 81	10"	K	10.2 ± 1.1	151 ± 2.9	16.4 ± 0.5	
	4 May 81	10"	K	6.6 ± 4.9	23 ± 20	14.2 ± 0.9	
1514-241 (AP Lib)	4 May 81	10"	K	2.8 ± 2.3	179 ± 22	25.5 ± 0.5	
	4 May 81	10"	H	6.0 ± 2.1	132 ± 10	22.0 ± 0.4	
1641+399 (3C 345)	5 Apr 81	10"	K	6.4 ± 1.4	120 ± 6.0	18.3 ± 0.6	
	6 Apr 81	10"	K	11.3 ± 1.5	108 ± 3.6	19.3 ± 0.6	
	7 Apr 81	10"	K	8.1 ± 0.9	118 ± 3.0	18.6 ± 0.6	
	8 Apr 81	10"	K	6.8 ± 1.5	101 ± 6.0	20.8 ± 0.6	
			H	11.7 ± 0.9	96 ± 2.1	12.7 ± 0.3	
	30 Apr 81	10"	K	16.2 ± 1.2	148 ± 2.0	15.2 ± 0.5	
			H	14.7 ± 3.6	152 ± 4.8	9.3 ± 0.5	
	1 May 81	10"	K	11.6 ± 2.3	86 ± 3.8	14.9 ± 0.4	
			H	11.4 ± 3.4	95 ± 4.8	8.8 ± 0.4	
	2 May 81	10"	K	8.8 ± 1.9	99 ± 5.9	13.6 ± 0.4	
	3 May 81	10"	K	7.3 ± 3.8	91 ± 10	10.6 ± 1.6	
	4 May 81	10"	K	3.3 ± 1.7	84 ± 14	9.1 ± 0.5	
	2200+420 (BL Lac)	1 May 81	10"	K	10.6 ± 0.8	3.3 ± 2.1	51.3 ± 1.5
				H	15.1 ± 3.5	2.1 ± 6.3	26.4 ± 1.3
2 May 81		10"	K	14.2 ± 0.8	9.7 ± 1.5	57.2 ± 1.7	
			H	14.9 ± 2.2	4.8 ± 2.7	31.2 ± 1.6	
			J	11.3 ± 1.6	4.4 ± 2.9	22.8 ± 0.5	
3 May 81		10"	K	4.2 ± 1.1	6.5 ± 7.2	103.2 ± 15.4	
4 May 81		10"	K	9.8 ± 1.1	20.6 ± 3.1	38.9 ± 1.9	
	H		8.1 ± 0.9	21.9 ± 3.0	28.5 ± 1.5		

Table 1 – continued

(1) Object	(2) Date	(3) Aperture	(7a) {S ± σ(S)} _K	(7b) {S ± σ(S)} _H	(7c) {S ± σ(S)} _J
0235+164 (AO)	10 Jul 80	15"	9.2 ± 0.1	—	—
	9 Aug 80	19"	11.8 ± 0.3	6.3 ± 0.5	—
	10 Aug 80	15"	12.6 ± 0.4	7.1 ± 0.6	4.6 ± 0.4
	11 Aug 80	15"	—	6.4 ± 0.4	4.2 ± 0.3
0754+101 (OI 090.4)	7 Apr 81	10"	—	10.5 ± 0.3	5.7 ± 0.2
	8 Apr 81	10"	—	11.0 ± 0.2	8.5 ± 0.2
0818-131 (OJ -131)	8 Apr 81	10"	—	9.3 ± 0.2	7.2 ± 0.1
0851+202 (OJ 287)	12 Mar 81	7.5"	22.9 ± 1.1	15.1 ± 0.8	11.0 ± 0.6
	13 Mar 81	7.5"	33.7 ± 1.7	24.8 ± 1.2	17.6 ± 0.9
	14 Mar 81	7.5"	28.1 ± 1.4	20.5 ± 1.0	14.0 ± 0.7
	8 Apr 81	10"	—	12.3 ± 0.2	9.7 ± 0.3
0912+297 (OK 222)	7 Apr 81	10"	6.3 ± 0.3	4.3 ± 0.3	3.8 ± 0.2
	8 Apr 81	10"	—	4.9 ± 0.3	3.6 ± 0.1
1147+245 (OM 280)	20 Apr 80	15"	—	6.1 ± 0.1	—
	21 Apr 80	10"	9.1 ± 0.2	5.7 ± 0.2	—
1156+295 (4C 2945)	8 Apr 81	10"	—	—	19.7 ± 0.6
	30 Apr 81	10"	—	5.6 ± 0.2	3.8 ± 0.2
	2 May 81	10"	—	7.9 ± 0.2	5.7 ± 0.2
	3 May 81	10"	—	9.9 ± 0.3	6.6 ± 0.2
	4 May 81	10"	—	6.1 ± 0.2	4.2 ± 0.2
1253-055 (3C 279)	7 Apr 81	10"	—	3.4 ± 0.2	—
	8 Apr 81	10"	—	3.7 ± 0.2	—
	3 May 81	10"	2.0 ± 0.4	1.7 ± 0.3	0.8 ± 0.2
	4 May 81	10"	2.6 ± 0.1	1.9 ± 0.1	1.2 ± 0.2
1308+326 (B2)	20 Apr 80	15"	—	2.6 ± 0.2	2.0 ± 0.2
	6 Apr 81	10"	1.1 ± 0.1	0.7 ± 0.1	—
	8 Apr 81	10"	1.0 ± 0.1	—	—
	3 May 81	10"	—	6.6 ± 0.7	5.3 ± 0.5
	4 May 81	10"	—	5.7 ± 0.1	4.8 ± 0.4
1335-127 (PKS)	3 May 80	8"	17.6 ± 0.5	—	6.7 ± 0.2
	7 May 81	10"	4.3 ± 0.2	2.3 ± 0.2	—
1400+162 (OQ 100)	7 May 81	10"	3.6 ± 0.2	2.5 ± 0.2	—
1418+546 (OQ 530)	20 Apr 80	15"	—	—	6.2 ± 0.3
	21 Apr 80	10"	12.9 ± 0.2	10.1 ± 0.3	—
	2 May 81	10"	—	8.0 ± 0.2	5.0 ± 0.1
	4 May 81	10"	—	10.7 ± 0.2	7.7 ± 0.2
1514-241 (AP Lib)	18 Apr 81	10"	—	—	15.5 ± 0.7
	4 May 81	10"	—	—	16.3 ± 0.3
1538+149 (4C 14.60)	2 May 81	10"	1.7 ± 0.1	1.3 ± 0.1	1.0 ± 0.1

Table 1 – continued

(1) Object	(2) Date	(3) Aperture	(7a) {S ± σ(S)} _K	(7b) {S ± σ(S)} _H	(7c) {S ± σ(S)} _J
1641+399 (3C 345)	7 Apr 81	10"	—	11.8 ± 0.2	8.1 ± 0.2
	8 Apr 81	10"	—	—	8.7 ± 0.2
	2 May 81	10"	—	8.0 ± 0.2	5.0 ± 0.1
	4 May 81	10"	—	5.3 ± 0.2	3.6 ± 0.1
1727+503 (I Zw 187)	8 Apr 81	10"	4.6 ± 0.2	3.3 ± 0.2	—
1749+096 (OT 081)	30 Apr 81	10"	4.3 ± 0.1	2.9 ± 0.1	1.4 ± 0.1
1921-293 (OV -236)	20 Apr 80	15"	—	3.8 ± 0.1	—
	21 Apr 80	10"	5.5 ± 0.1	—	—
	9 Jul 80	15"	4.6 ± 0.1	3.9 ± 0.2	—
	30 Apr 81	10"	5.6 ± 0.2	3.8 ± 0.1	2.6 ± 0.2
	1 May 81	10"	6.9 ± 0.1	4.0 ± 0.2	2.6 ± 0.2
	2 May 81	10"	6.5 ± 0.1	4.2 ± 0.2	2.9 ± 0.1
	4 May 81	10"	7.5 ± 0.3	5.0 ± 0.3	3.2 ± 0.2
2155-304 (PKS)	9 Aug 80	15"	34.8 ± 1.0	29.0 ± 1.8	28.5 ± 2.2
	10 Aug 80	15"	37.9 ± 1.1	31.7 ± 2.0	—
	11 Aug 80	15"	40.0 ± 1.0	34.2 ± 2.6	28.5 ± 1.8

vation and columns (3) and (4) contain the aperture size and waveband of the measurement. The degree of polarization, position angle and flux in millijansky ($1\text{mJy} = 10^{-29}\text{Wm}^{-2}\text{Hz}^{-1}$) are contained in columns (5), (6) and (7) along with their associated rms errors. The final part of Table 1 contains photometry alone, with flux measurements at K , H and J in columns (7a, b and c).

3.1 0818 – 128

OJ-131 is the Ohio Radio source with a flat spectrum which was identified with a blue polarized object by Tapia *et al.* (1977). Tapia *et al.* list radio fluxes from 408 MHz to 10.8 GHz, and they also mention the lack of emission lines visible in low-dispersion spectra. The linear polarization in the optical region was very high and variable (9–36 per cent). OJ-131 has a range of variability of 2.9 mag (Craine, Duerr & Tapia 1978), and at peak flux is one of the optically brightest BL Lac objects known. Optical polarimetry by Angel *et al.* (1978) over a two month period gave a range of 12–25 per cent at polarization position angles of 60–95°. Infrared monitoring shows it to have moderate infrared polarization (9–14 per cent) and a shallower infrared continuum than is normal for a BL Lac object ($\alpha \approx 0.7$, where $S(\nu) \propto \nu^{-\alpha}$). There were flux variations of up to 15 per cent on successive nights.

3.2 1156 + 295

4C 29.45 is a variable compact source with a flat spectrum from 178 MHz–5 GHz (Conway *et al.* 1974). It is identified with a strong-lined quasar at $z=0.728$ (Schmidt 1974), which has strong optical polarization of up to 10 per cent with no preferred position angle. The optical brightness varies by at least two magnitudes (Moore & Stockman 1981). 4C 29.45 was the subject of widespread interest during early 1981 because it was undergoing a dramatic flare at optical/infrared wavelengths.

The UKIRT monitoring covered a 4 day run in 1981 April and a 5 day run in May 1981. At the beginning of April the source was at the peak of its flare, with an enormous $2.2 \mu\text{m}$ flux of 75 mJy ($K=9.87$) and a strong infrared excess ($J-K=1.61$). When the non-thermal component was at its strongest, there was no evidence for wavelength dependent polarization between J , H , and K bands. Thereafter, the $2.2 \mu\text{m}$ flux fell by a factor of 2.3 in only three days. The infrared polarization followed the flux, rising to 14 per cent (K) at the time of peak flux and then falling to 5 per cent two days later. During these same four days the position angle rotated by approximately 50° . By the end of the month, the flare had subsided. On April 30, the $2.2 \mu\text{m}$ flux was down by a factor of 8.6 from its peak of three weeks earlier. The polarization was still highly variable from night to night, and the position angle swung by large amounts (up to 50°) from night to night. Unfortunately in the faint phase there was not sufficient signal-to-noise to study wavelength-dependent polarization. The polarization behaviour of 4C 29.45 was even more erratic in its low-flux state than in its high-flux state. These infrared measurements were part of a multi-wavelength collaboration on this object (Glassgold *et al.* 1983).

3.3 1253 – 055

This source is one of the optically violent variable (OVV) quasars, with strong emission lines and a history of large-amplitude optical variability. 3C 279 is in fact the most variable extra-galactic source known, varying by over 6.7 mag (Eachus & Liller 1975). At peak brightness it is one of the most luminous objects in the universe ($z=0.536$). 3C 279 is a strong X-ray emitter (Tananbaum *et al.* 1980), and shows a steep power-law continuum of slope $\alpha=1.3$ in the range $1-10 \mu\text{m}$ (Rieke *et al.* 1977). The radio properties of 3C 279 are intriguing. It has a compact variable source which has been extensively studied by VLBI techniques (Cotton *et al.* 1979; Kellerman *et al.* 1971). The fringe visibilities change with time, which implies a superluminal velocity of $\sim 21c$ for the compact components (Seielstad *et al.* 1979; Cotton *et al.* 1979). Optical polarimetry of 3C 279 has been published by Visvanathan (1973), Kinman (1967) and Elvius (1968), and the range is 4–19 per cent with large variations in position angle. These are the first published infrared measurements, and they show high polarization at $2.2 \mu\text{m}$ and variability by a factor of 3 over a one-month period. The infrared spectral index ($\alpha=1.4-1.7$) agrees with previous optical and infrared measurements.

3.4 1335 – 127

This is an object from the Parkes 2.7 GHz flat spectrum sample (Condon, Hicks & Jauncey 1977) which was shown to be a very red source ($\alpha \approx 3.0$) by Impey & Brand (1981). Aller, Aller & Hodge (1981) have monitored the radio polarization at 14.5, 8.0 and 4.8 GHz and find variability in both the flux and polarization at these frequencies. There is evidence for differential rotation between the position angles at high and low frequencies. Two flux measurements at $2.2 \mu\text{m}$, separated by almost a year, show large amplitude variability by over a factor of 4. The source has so far been too faint to attempt a polarization measurement.

3.5 1538 + 149

4C 14.60 has a large variability amplitude of > 2.8 magnitudes (Usher 1975) and a steep and variable spectral index in the optical region (Tapia *et al.* 1977). Kinman (1976) has made

a single optical polarization measurement of 22 per cent and Wills *et al.* (1980) have measured values in the range 17–20 per cent. Infrared photometry at J , K and K shows a spectral index $\alpha \approx 0.9$, which is considerably flatter than the optical slope. The difference is more than can be accounted for by a break in the spectrum due to synchrotron losses. 4C 14.60 has no published redshift.

3.6 1749 + 096

OT081 has a range of optical polarization of 3–9 per cent (Kinman 1976) and it has a steep optical continuum of spectral index $\alpha = 2.2$ (Tapia *et al.* 1977). The source has no emission line redshift. Wills *et al.* (1980) have made optical polarization measurements in the range 4–12 per cent. The spectral index from the infrared measurements ($\alpha \approx 2.0$) is in close agreement with the optical data. If the source has no large amplitude variability, then the inferred $V-K$ value is 4.0, which is typical for BL Lac objects.

3.7 2200 + 420

The prototype object BL Lacertae was thought for many years to be a variable star, until it was identified with the radio source VR0 42.22.01 (Schmitt 1968; MacLeod & Andrew 1968). BL Lac has been extensively studied and its properties have been reviewed by Stein, O'Dell & Strittmatter (1976) and Miller (1978). The non-thermal source has now been demonstrated convincingly to lie at the centre of a giant elliptical galaxy at $z = 0.07$ (Miller & Hawley 1977; Miller *et al.* 1978). The optical polarization of BL Lac varies from 2–23 per cent and over all position angles (see e.g. Angel *et al.* 1978). In addition, simultaneous optical/infrared polarimetry has been published by Knacke, Capps & Johns (1976) and Puschell & Stein (1980), and near-simultaneous polarimetry from centimeter to visual wavelengths has been obtained by Rudnick *et al.* (1978). However, the most impressive results have been achieved by a world-wide collaboration which monitored BL Lac almost continuously for a week in 1978 (Moore *et al.* 1982). This group found the Stokes parameters Q and U to vary quasi-periodically on a time-scale of ~ 1 day, with a superimposed longer time-scale variation involving a rotation of the position angle. Where infrared points were available they tracked the optical polarization and position angle.

In four nights of observation in 1981 May, BL Lac showed erratic polarization behaviour with variations of up to 10 per cent between successive nights. On the other hand, the position angle was stable $\pm 5^\circ$. There was no evidence for wavelength dependent polarization during that period. The flux variations were very large, and the $2.2 \mu\text{m}$ flux reached a peak of 103 mJy ($K=9.5$), after which it fell by a factor of 2.6 in *only* 24 hours. This is one of the largest brightness changes ever recorded in a BL Lac object, and is rivalled only by an optical change of a factor of 2.5 in 24 hours reported in BL Lac by Veron (1978). It is clear that these dramatic variations are not sampled from the same sort of light curves that were observed in 1979 September.

3.8 OTHER OBJECTS

(1) 0735 + 178 was well-observed during 1981 April/May, during which time the object went through a broad flux and polarization flare. The $2.2 \mu\text{m}$ flux and polarization went from ~ 18 mJy and ~ 12 per cent in early April to ~ 28 mJy and ~ 25 per cent in early May. Between the nights of April 6 and 7 there was a 25° position angle rotation, seen at two different wavelengths. (2) Over a five night period, the $2.2 \mu\text{m}$ polarization of 0754 +

101 fell from 19 per cent to 3 per cent only a 10 per cent change in the total flux. The position angle was roughly constant. (3) 0912 + 297 was shown to have high infrared polarization for the first time, with moderate (~ 15 per cent) variability of its infrared flux. (4) 1308 + 326 again demonstrated rapid polarization changes (~ 10 per cent in 24 hours), but at a completely different position angle from previous measurements. (5) There were also large position angle rotations in 1418 + 546, when the position angle changed by $\sim 50^\circ$ in two days. (6) 16 + 1 + 399 was interesting because over a five day period there was a smooth monotonic decrease in both degree of polarization and infrared flux.

4 Discussion

Together with Paper I, this paper brings the number of BL Lac objects we have measured up to 25, 19 of which have been measured polarimetrically in the infrared, 10 for the first time. The principal wavelength of the study was $2.2 \mu\text{m}$, but 13 objects have polarimetry at shorter wavelengths also. 15 of the BL Lac objects in the sample have redshifts, so useful (but model-dependent) physical information can be derived for them. Although BL Lac objects generally have featureless continua, spectra with good signal to noise ratio have revealed weak emission and absorption lines in many objects. For the purpose of this work OVV quasars are included in the sample since they share the properties of the BL Lac compact source: variability, polarization and a steep infrared continuum.

The sample includes nearly half of the objects in the compilation by Angel & Stockman (1980), and it is probably large enough for the data to be considered representative of the infrared properties of BL Lac objects. However, there are clearly selection effects operating. Since techniques involving slitless spectroscopy and searches for UV excess are not appropriate for BL Lacs, most have been found from accurate positions of flat spectrum radio sources. There is currently *no* known example of a radio-quiet BL Lac object, and it is possible that this absence is not simply a selection effect. For example, BL Lac objects are intrinsically strong radio emitters compared to quasars, and most BL Lacs selected by non-radio properties have turned out to be radio-emitters. The question may be answered by studies currently under way which select objects by their optical polarization variability and X-ray emission (Borra, 1983; Hawkins 1983; Impey & Brand 1982; Stocke *et al.* 1982; Chanan *et al.* 1982). A more serious problem for this study is the fact that radio source identification procedures select against strong infrared-emitters (Rieke & Lebofsky 1979). For example, if a sample of flat spectrum sources is observed in the infrared without regard to optical identification, there is a smooth distribution of near-infrared spectral indices from $\alpha=0$ to $\alpha=3$ (where $S(\nu) \propto \nu^{-\alpha}$). Some of the reddest objects are BL Lac objects (Impey & Brand 1981). However, the spectral index distribution of the sample of BL Lac objects peaks around $\alpha=1.5-1.7$ and drops off for sources with spectra steeper than $\alpha \approx 2$ (next section), so the very red objects are clearly being missed.

4.1 SPECTRAL ENERGY DISTRIBUTION

The near-infrared continuum in BL Lac objects is presumed to be due to synchrotron radiation from relativistic electrons. The two most compelling reasons for this assumption are the high polarization in BL Lac objects, and the continuity of the infrared flux with the high frequency radio spectrum, where the synchrotron interpretation is secure. Thus, the infrared flux is interpreted as the high energy tail of the compact radio component. However, this latter interpretation is not at all secure (BL Lac: Rieke & Kinman 1974, 1413 + 135; Beichman *et al.* 1981, 0235 + 164; Rieke *et al.* 1976).

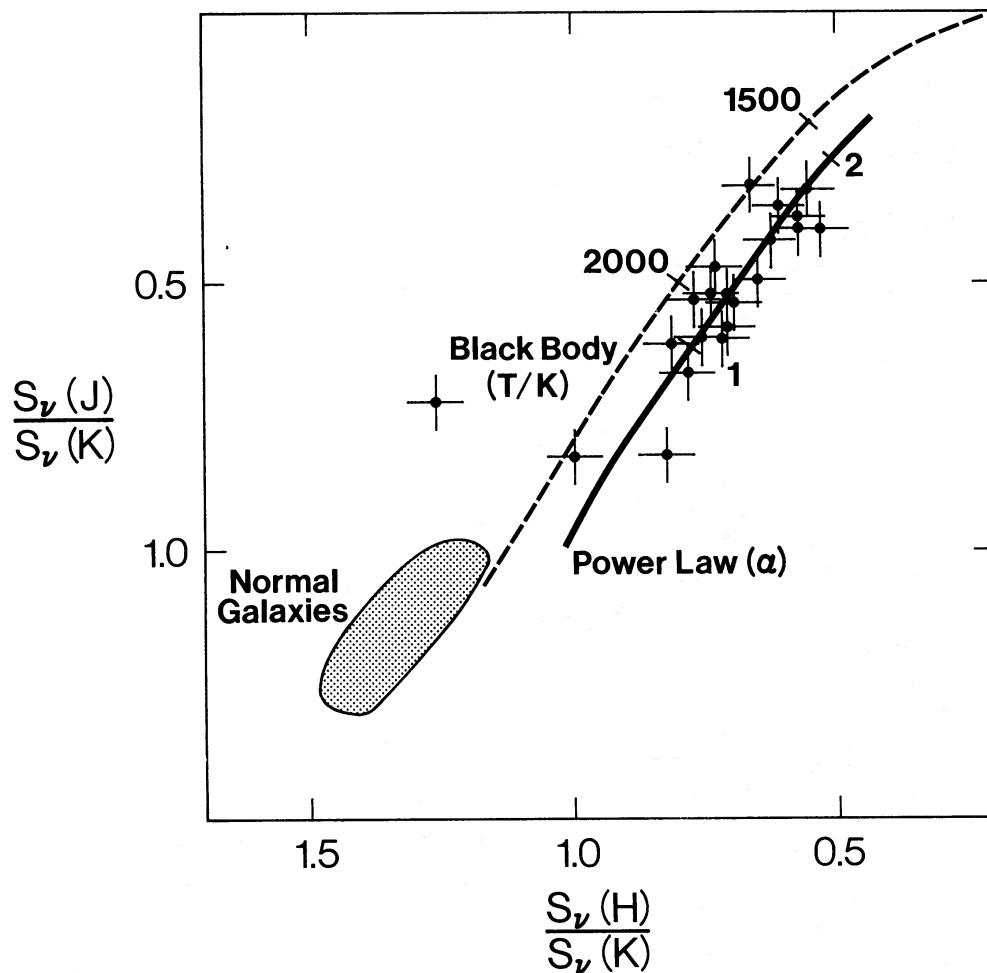


Figure 1. Infrared flux ratios are plotted for 21 BL Lac objects based on photometry at J , H and K . The region of colours for normal (elliptical) galaxies is shown as a shaded area, and the two loci of black-body and power-law spectra are marked in units of temperature and spectral index respectively.

A major aim of this work is to understand the polarization and flux properties of the central regions of BL Lac objects. Therefore, we must be sure that the infrared measurements are isolating the non-thermal component. A relatively model-free way of doing this is to use a two-colour plot. It is noted that flux ratios and two-colour diagrams are very appropriate for studying composite systems (Becker 1937; Wade 1980).

In Fig. 1, infrared flux ratios are plotted for 21 BL Lac objects. For objects where more than one set of measurements was made, we plotted the data set which is nearest the object's mean spectral index. Two lines are superimposed, one of which is the locus of blackbody colours (with temperature marked), and the other of which is the locus of power-law spectra (with spectral index marked). The area corresponding to the colours of normal elliptical galaxies is defined from the work of Frogel *et al.* (1978). Most of the sample lie close to the power-law line and a power law is a very good representation of the near-infrared spectral shapes. In fact, the scatter about the line is consistent with the photometric errors, and there is no need to invoke any other component. All but three objects fall in the range corresponding to $0.8 < \alpha < 1.8$. The three BL Lacs lying outside this range (Mk 501, 1727 + 503 and 2155 - 304) all have nonstellar images on deep, direct plates. Therefore, their colours are probably affected by the presence of an underlying galaxy component. Even three of the objects without three-colour photometry can be included in this argument, since their two-

colour ratios of $S(H)/S(K) = 0.53, 0.63, 0.68$ put them far into the non-thermal region of Fig. 1.

4.2 LUMINOSITY PARAMETERS

The calculation of near-infrared luminosity assumes (1) the cosmological nature of the redshift and (2) isotropic emission. Fifteen of the sample have published redshifts. The luminosity density in the rest frame of the BL Lac object is calculated from

$$L(\nu) = 4\pi \left(\frac{cz}{H_0} \right)^2 (1+z)^{-1} F[\nu/(1+z)]$$

assuming a Friedmann model with cosmological constant $\Lambda=0$ and taking $H_0 = 75 \text{ km s}^{-1} \text{ Mpc}^{-1}$ and $q_0 = 1$. As in Paper I, observed $2.2 \mu\text{m}$ fluxes are converted into BL Lac rest frame fluxes by $F[\nu/(1+z)] = F(\nu) (1+z)^\alpha$ where α is the near-infrared spectral index from $1-2 \mu\text{m}$. Table 2 shows the object name (1), redshift (2), luminosity distance (3), the maximum $1-2 \mu\text{m}$ luminosity observed (4), the number of observations of each object (5). The infrared luminosities are lower limits in almost all cases since only limited infrared bandwidths have been used. For a bandwidth of $1-10 \mu\text{m}$ and a typical spectral index of $\alpha > 1.4$, the integrated IR luminosity is increased by an order of magnitude, assuming no synchrotron turnover out to $10 \mu\text{m}$. The range of luminosity within the sample is very large: a factor of 1.2×10^3 .

Generating these prodigious luminosities is a problem for almost any power source. One of the reasons that the relativistic jet models are so popular is that they ease the lumin-

Table 2. Luminosities and their variations for 15 BL Lac objects.

(1)	(2)	(3)	(4)	(5)	(6)
Object	z	d(Mpc)	$L_{\text{MAX}}^{\text{IR}}$ (erg/sec)	$L_{\text{MAX}}/L_{\text{MIN}}$	No. Obsn.
0235+164	0.852	3410	4.8×10^{46}	5.0	12
0735+178	0.424	1700	2.3×10^{46}	3.4	18
0851+202	0.306	1220	1.4×10^{46}	2.5	11
1156+295	0.729	2920	9.6×10^{46}	6.5	9
1253-055	0.538	2150	7.5×10^{45}	3.2	6
1308+326	0.996	3980	3.2×10^{46}	11.7	10
1400+162	0.244	970	1.2×10^{45}	2.4	3
1514-241	0.049	200	4.8×10^{44}	1.1	2
1641+399	0.595	2380	2.8×10^{46}	2.9	11
1652+398	0.034	140	3.1×10^{44}	1.2	2
1727+503	0.055	220	7.9×10^{43}	1.6	7
1921-293	0.353	1410	4.5×10^{45}	1.6	7
2155-304	0.170	680	6.9×10^{45}	3.2	8
2200+420	0.069	280	4.2×10^{45}	3.1	4
2223-052	1.404	5620	5.1×10^{46}	2.0	5

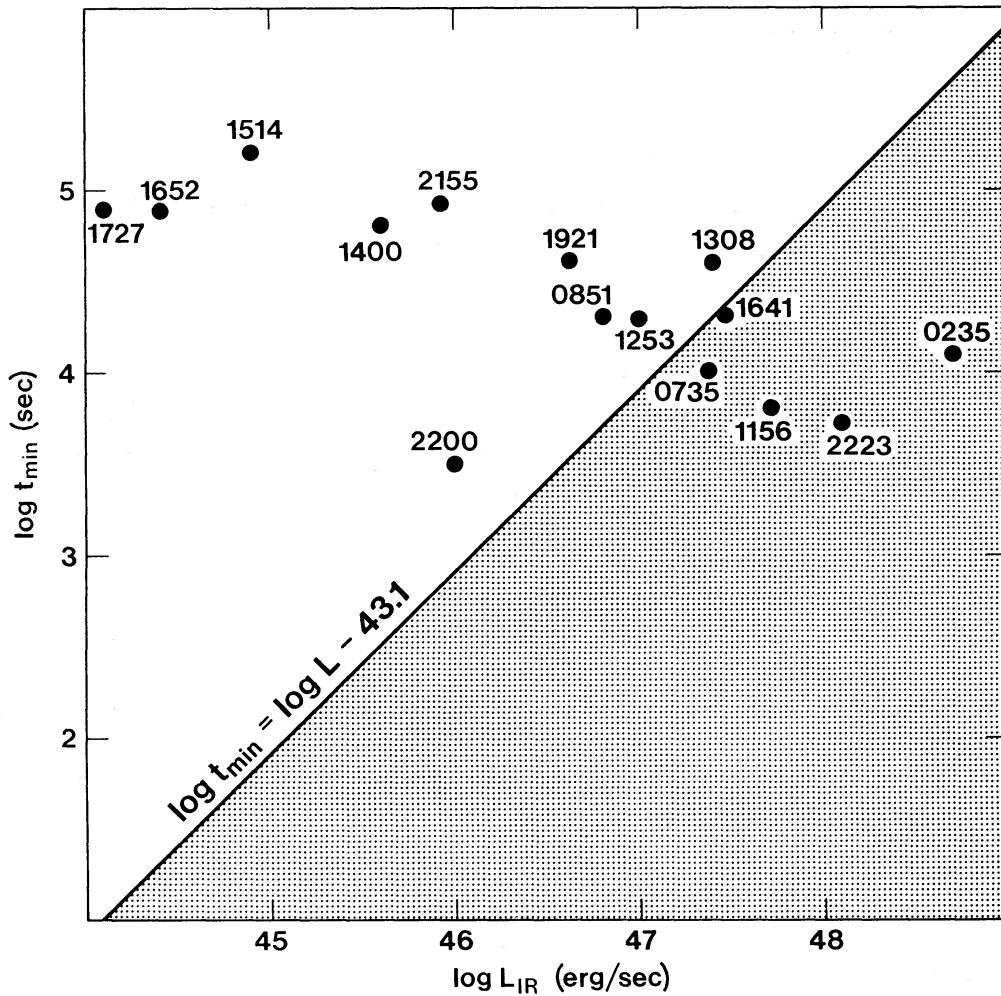


Figure 2. The maximum infrared luminosity is plotted against the minimum variability time-scale in the source rest frame. The shaded area corresponds to the forbidden zone of variability for a spherically accreting supermassive object (from Elliot & Shapiro 1974). A bandwidth of $1\text{--}10\ \mu\text{m}$ is used for the infrared luminosity. Values of t_{MIN} are normalized to variations of 10 per cent in intensity. Objects are labelled by the first four digits of their Parkes-type position designators.

osity requirements in compact sources. The size of the power source is inferred from the minimum variability time-scale in the BL Lac rest frame $t_{\text{VAR}}/(1+z)$, where $t_{\text{VAR}} = L/(dL/dt)$. A plot of $t_{\text{VAR, min}}$ versus the $1\text{--}10\ \mu\text{m}$ luminosity (data combined with paper I) now has *five* objects which violate the spherical accretion limit providing support for non-spherical accretion and jet emission (Fig. 2). The objects in question are BL Lac, A0 0235 + 164, B2 1308 + 326, 3C 446 and 1641 + 399. Note that in Figure 2, the values of t_{MIN} are normalized to variations of 10 per cent in intensity, so that the different rates and amplitudes of variability in BL Lac objects are dealt with uniformly.

We can investigate the dependence of source polarization and variability properties on luminosity. The sample is quite small, because it includes only those sources with redshifts and must exclude Mk 501, 1727 + 503 and 2155 – 304 in order to rule out objects with thermal dilution. All the measured quantities (flux, polarization, position angle, spectral index) vary by large amounts for a *given* object, and this can swamp the trends between objects unless the parameters are carefully chosen. For example, maximum and mean luminosities may probe different physical regions (if relativistic jet models apply, the

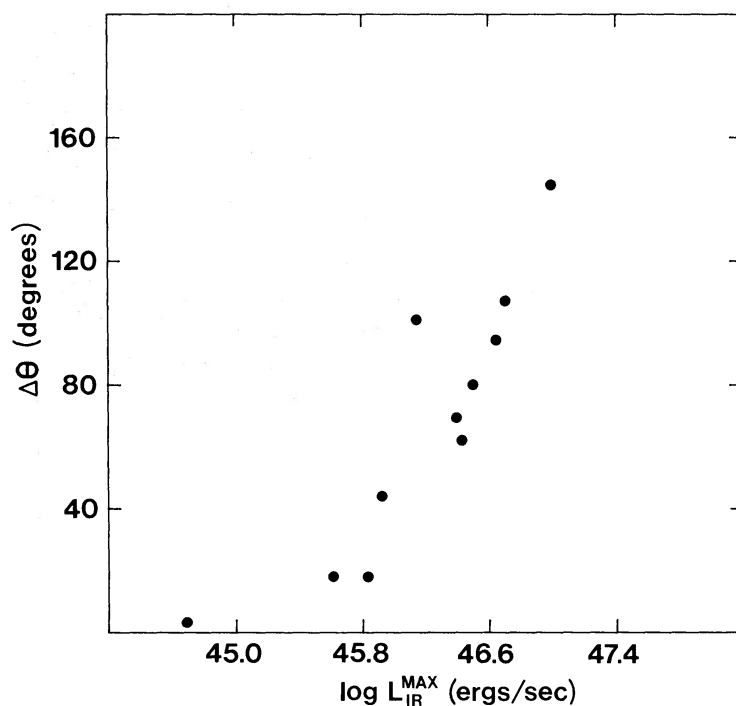


Figure 3. Range of position angles from the accumulated monitoring plotted against the peak infrared luminosity.

mean luminosity might be emission from the bulk of the jet, while the peak luminosity is emission from knots or condensations within the jet). There are no significant correlations between the maximum $1-2\ \mu\text{m}$ luminosity and either the (1) maximum degree of polarization, (2) the range of polarization, (3) the variability index (defined by L_{MAX}/L_{MIN}), (4) the maximum $1-2\ \mu\text{m}$ spectral index or (5) the mean $1-2\ \mu\text{m}$ spectral index. (There is a possible correlation between mean spectral index and mean luminosity, but only at the $1.8\ \sigma$ level in a sample of 12 objects.). However, somewhat surprisingly, the range of position angles for an object does correlate with the luminosity. Fig. 3 shows the plot, and the Spearman non-parametric estimator gives a rank correlation of 0.86, which means that the parameters are related at the 99 per cent confidence level. Removing any subset of BL Lacs does not destroy the correlation; nor does plotting mean luminosity instead of peak luminosity. Only part of the correlation is due to the selection effect of more frequently observed objects showing larger values of position angle rotation. The relative error in the $1-10\ \mu\text{m}$ luminosity of Fig. 2 can be shown to be little larger than the relative error in the photometry, given in Table 1. This assumes no dramatic breaks in the spectral shapes of these objects.

This relationship is important because it connects the luminosity of a BL Lac object with a luminosity-independent parameter. The range of position angle is a purely geometrical quantity. For synchrotron radiation in the infrared, the source is optically thin and plasma propagation and Faraday effects can be ignored. In this regime, the position angle of polarization reflects the component of the magnetic field perpendicular to the line-of-sight. There are two ways to interpret large position angle variations. Either there is a large scale rotation of the field embedded in the emitting volume; or the field makes a small angle to the line of sight, so that the projection of small changes in a field direction results in large rotations of position angle.

4.3 RELATIONSHIP BETWEEN POLARIZATION, AND SPECTRAL INDEX

A general link between high degree of polarization, large amplitude variability and steep infrared spectrum was discussed in Paper I. There is a clear separation between the properties of BL Lac objects and radio-loud quasars, since most radio-loud quasars do not have high polarization (Stockman & Angel 1978), large amplitudes of variability (Bonoli *et al.* 1979), or steep infrared spectra (Neugebauer *et al.* 1979). As part of a unified picture of active nuclei, Blandford & Königl (1979) have proposed a model where much of the non-thermal radiation comes from a relativistic jet. They envisage a sequence of increasing activity (radio-quiet quasar, radio-loud quasar, OVV quasar, BL Lac object) corresponding to smaller and smaller angles of the jet axis wrt. the line-of-sight. In Paper I, a good correlation was

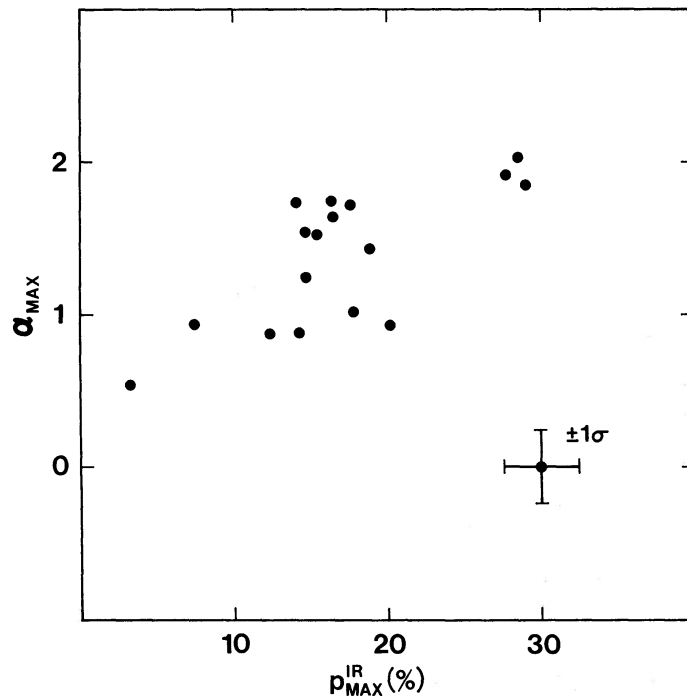


Figure 4. Infrared spectral index plotted against maximum 2.2 μm polarization.

found between maximum infrared polarization and maximum 2.2 μm spectral index for 14 BL Lac objects. With more data on each object, and a slightly increased sample of 17 (it also becomes possible to standardize on K polarization), the correlation is still evident (see Fig. 4). The expanded data set gives a Spearman correlation of 0.68, and so the variables are related at the 95 per cent confidence level. The data are listed in Table 3, which contains the object name (1), the maximum 2.2 μm polarization (2), the maximum optical polarization (3), the optical variability amplitude (4), and the mean 1–2 μm spectral index (5). The numbers in column 4 are taken from Angel & Stockman (1980).

The quantities $p_{\text{MAX}}^{\text{IR}}$ and α_{MAX} may be indirectly related, through a third parameter (N), which is the number of observations. For any observable with an arbitrary distribution of values about the mean, the maximum measured value increases as the number of measurements increases (in the case of a Gaussian parent distribution, it increases as \sqrt{N}). Plots of N vs. $p_{\text{MAX}}^{\text{IR}}$ and N vs. α_{MAX} do in fact show a very slight correlation, but the correlation between $p_{\text{MAX}}^{\text{IR}}$ and α_{MAX} is too strong to be the result of a selection effect (the correlation still has a similar scatter if $\overline{p_{\text{MAX}}^{\text{IR}}}$ and $\overline{\alpha}$ are used instead of peak values).

A relationship between $p_{\text{MAX}}^{\text{IR}}$ and α_{MAX} with such a steep slope is intriguing because it connects two parameters closely related to the geometry of the source. We note that the

Table 3. Maximum polarization, variability, spectral index.

(1)	(2)	(3)	(4)	(5)
Object	IR p_{MAX}	OPT p_{MAX}	ΔB	$\bar{\alpha}_{\text{IR}}$
0235+164	36.2	44	5.2	2.1
0306+103	3.6	—	2.2	—
0735+178	32.6	31	2.5	1.2
0754+101	18.9	26	1.0	0.95
0818-131	21.4	36	2.9	0.78
0851+202	19.7	32	4.0	1.0
0912+297	12.2	13	1.9	0.99
1147+245	14.8	13	1.4	1.4
1156+295	15.3	9	2.6	1.2
1253-055	17.6	19	6.7	1.5
1308+326	20.1	25	5.6	0.92
1335-127	—	—	—	1.7
1400+162	—	14	—	1.2
1418+546	17.9	19	4.8	1.0
1514-241	7.4	7	2.5	0.86
1538+149	—	22	2.8	0.92
1641+399	16.2	16	2.0	1.6
1652+398	—	4	0.5	0.36
1727+503	—	6	1.9	1.0
1749+096	—	9	—	2.0
1921-293	13.9	8	2.5	1.5
2155-304	3.0	7	—	0.35
2200+420	15.1	23	4.0	1.6
2223-052	16.3	17	3.4	1.5
2254+074	17.4	21	1.6	—

slope is too steep to be due simply to the variation of p with α in simple partially aligned field models.

$p_{\text{MAX}}^{\text{IR}}$ is a measure of the maximum degree of alignment of the magnetic field in the synchrotron-emitting region ($p_{\text{MAX}} \propto (B_{\parallel}^2 - B_{\perp}^2)/B^2$, where B_{\parallel} and B_{\perp} are the field components resolved parallel and perpendicular to the line-of-sight). For a single synchrotron component with a uniform magnetic field, $p_{\text{MAX}} = (\alpha + 1)/(\alpha + 5/3)$. In some objects like 0235 + 164 and 0735 + 178 the values of p_{MAX} are a large fraction of the theoretical maximum value, implying that the integrated field over the whole emitting volume is nearly uniform. The steepest spectral index α_{MAX} indicates strong synchrotron losses, but could

also relate to the geometry of the source. Marscher (1980) has shown that the spectrum of an unresolved relativistic jet steepens as its angle to the line-of-sight decreases. One way of interpreting Fig. 4 is as a sequence of BL Lac objects with jets, where the steep spectrum, highly polarized sources have jets nearly pointing at the observer.

4.4 CHANGES IN POLARIZATION, VARIABILITY AND IR-EXCESS

There are 85 data points covering night-to-night variations ($\Delta t = 20\text{--}28$ hr) in the flux at $2.2\ \mu\text{m}$ and changes in the $1\text{--}2\ \mu\text{m}$ spectral index. Some of the transitions are highly significant, and they can all be dealt with as an ensemble because there are no selection effects biasing the distributions $n(\Delta S_K)$ and $n(\Delta\alpha)$. No systematic effects of the kind discussed by O'Dell *et al.* (1978) are found. Although these variations probe the smallest dimensions of the compact source, the synchrotron life-times of the highest energy electrons are short enough to affect the spectrum on a time-scale of a day. The spectral index is therefore probably determined by a balance between acceleration mechanism and synchrotron losses for the relativistic electrons.

In addition, changes in $2.2\ \mu\text{m}$ polarization and changes in the spectral index can be considered, giving 61 data points for night-to-night variations. A relationship has already been demonstrated between the quantities $p_{\text{MAX}}^{\text{IR}}$ and α_{MAX} . However, there is no correlation between changes in polarization and changes in spectral index. This null result is interesting because it indicates that the relationship between $p_{\text{MAX}}^{\text{IR}}$ and α_{MAX} is not simply a result of short-term energy injection into the source, but is connected with some fundamental (geometric) property of each BL Lac object.

The database of polarimetry and photometry from this paper and from Paper I is sufficient to investigate the amplitude of variability on different time-scales. The data was collected during seven separate runs covering an eighteen month period, and night-to-night changes are particularly well sampled. The evidence indicates that substantial variations on time-scales of less than a day are rare (but see Puschell *et al.* 1979; Stockman & Angel 1978; Snyder *et al.* 1980). After a large polarization monitoring programme, Angel *et al.* (1978) concluded that the spectrum of fluctuations falls off above $\nu \sim (\text{day})^{-1}$. Therefore, the night-to-night observations probe the smallest unit of emission in the active core of the objects. Additional run-to-run measurements have an average spacing of one month, which is a typical time-scale for the larger flares measured in long-term monitoring programmes (Epstein *et al.* 1982).

First, the distribution of polarization changes at $\Delta t \sim 1$ day can be compared with the polarization changes over the longer baseline $\Delta t \sim 1$ month. Although some of the polarization changes ($\Delta p, = p_2 - p_1$) are numerically small, an analysis of the relative error distribution shows that (1) the errors are distributed normally, and (2) the error distributions for night-to-night and run-to-run are identical. We use the Mann-Whitney U-Test, which is a non-parametric test and does not presume a form for the parent distribution. This test is then used to compare the distributions of Δp on day and on month time-scales. The resulting rankings show that the two distributions are identical at the 87 per cent confidence level. Second, the flux changes (ΔI) on day and month scales can be compared. The Mann-Whitney Test reveals that the monthly flux changes are longer than the night-to-night flux changes, at the 99.94 per cent confidence level. The mean level of ΔI for $\Delta t \sim 1$ month is a factor of 2.4 higher than the mean ΔI for $\Delta t \sim 1$ day. The relatively constant value of Δp is not due to p being a bounded parameter [i.e., $0 < p < (\alpha + 1)/(\alpha + 5/3)$ for synchrotron radiation], since the values of Δp cover a small fraction of the allowed range. While the amplitude of intensity variation in BL Lac objects increases from day to month time-scales, the amplitude of polarization variation is constant.

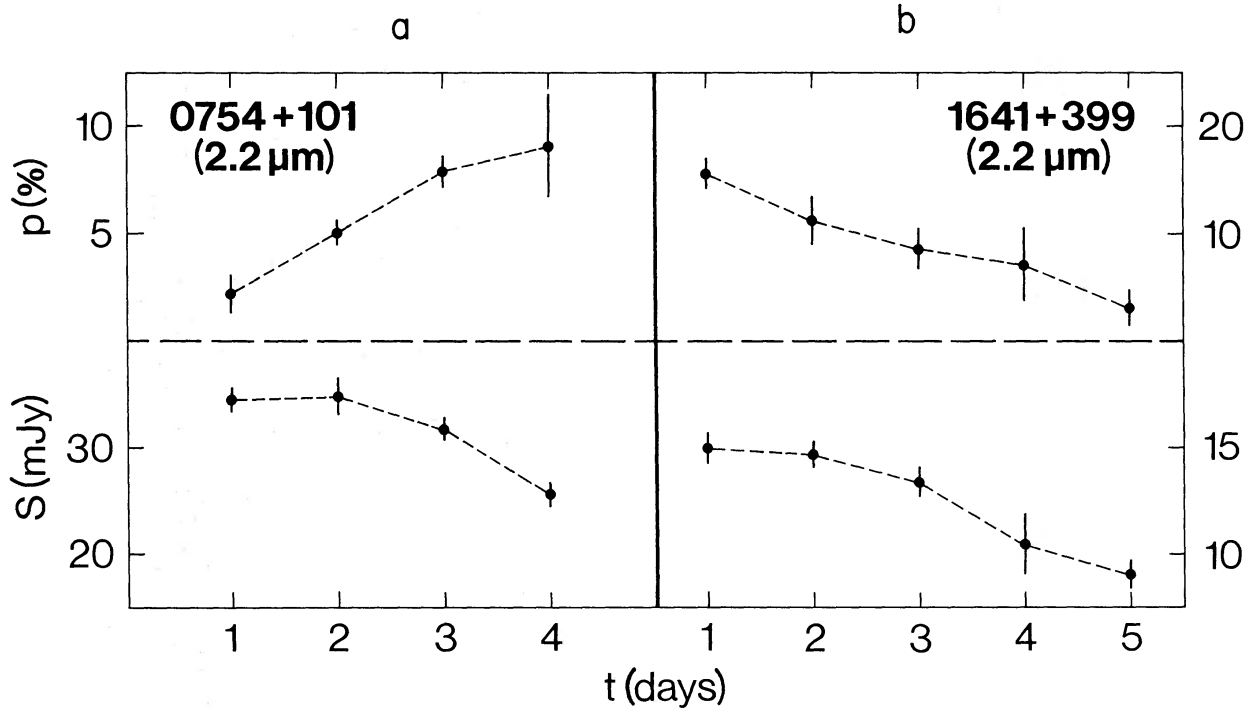


Figure 5. Degree of polarization and total flux at $2.2 \mu\text{m}$ are plotted for two objects monitored on several consecutive nights (a) 0754 + 101, (b) 1641 + 399.

4.5 CHANGES IN POLARIZED AND TOTAL FLUX

In Paper I it was found that the changes in polarized and unpolarized flux for two BL Lac objects could be understood in terms of a synchrotron component of variable flux and fixed polarization. On a diagram of ΔI_{TOT} vs. ΔI_{POL} , these objects had a strongly peaked or correlated distribution (where $\Delta I_{\text{TOT}} = I_2 - I_1$ and $\Delta I_{\text{POL}} = p_2 I_2 - p_1 I_1$). Other objects had changes in flux and polarization that were completely uncorrelated. Examples of monotonic behaviour are given in Figs 5a and b, where the flux and polarization are plotted for 0754 + 101 and 1641 + 399 over the period of a monitoring run. The two objects show an opposite sense of polarization and flux changes. This distribution can be reinvestigated now with much improved statistics: 85 data points compared to 41 in Paper I. Fig. 6 shows inter-night changes in the polarized and total flux plotted in absolute units. All objects with measurements on consecutive nights are included in the diagram and measurements in the J , H and K bands are combined.

One problem with interpreting the plot of ΔI_{TOT} vs. ΔI_{POL} is that the numerical values of ΔI_{POL} are low and the relative errors in the values of ΔI_{POL} are much higher than the relative errors in ΔI_{TOT} . Study of the distribution of individual errors shows that the errors in ΔI_{TOT} and ΔI_{POL} both have (a) similar, normal distributions, and (b) similar mean values of 0.3 mJy. A linear regression straight line can be fitted to the data for OJ 287 and 0735 + 178: $\Delta I_{\text{POL}} = 0.16 \Delta I_{\text{TOT}} - 0.03$ with coefficients of determination $R^2 = 0.57$. The value of

$$\chi^2 = \sum_i [(\Delta I_{\text{POL}})_i - 0.16 (\Delta I_{\text{TOT}})_i + 0.03]^2 = 24.0$$

for the straight-line fit can be compared with the value of

$$\chi^2 = \sum_i (\Delta I_{\text{POL}})^2 = 55.2$$

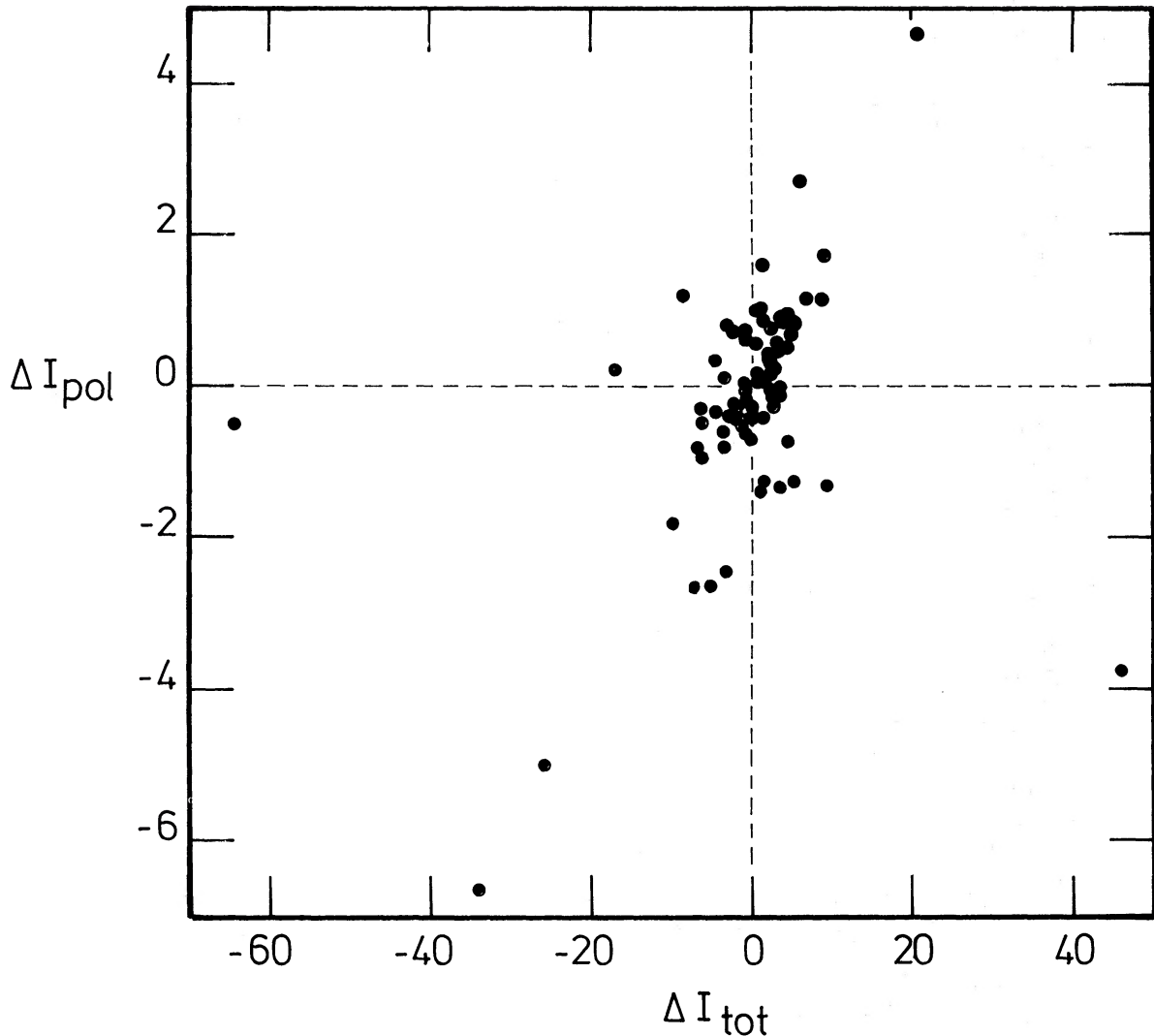


Figure 6. Inter-night changes in polarized flux are plotted against inter-night changes in total flux (both in absolute units). The mean standard errors in each axis are shown.

for the assumption that the values of ΔI_{POL} are scattered about the origin with no correlation (for 50 degrees of freedom). Therefore the data is inconsistent with

$$\frac{1}{n} \sum_i^n \Delta I_{\text{POL}} = 0$$

or a constant at the 95 per cent confidence level. Applying a non-parametric test gives the same conclusion. The Spearman Rank Correlation coefficient gives a probability of 99.5 per cent that the mean value of ΔI_{POL} is not zero, and depends on ΔI_{TOT} .

What produces the types of variation? Blandford & Rees (1978) have discussed consequences of polarization produced by n randomly oriented subunits (each ~ 70 per cent polarized). The degree of polarization is ~ 50 per cent/ \sqrt{n} and as one subunit is added or subtracted, the relative intensity, percentage polarization, and polarization angle change by $1/n$, $\sim 50/n$, and $1/\sqrt{n}$ radians respectively. The subunits vary on a time-scale of days, so their dimensions are $\sim 10^{15}$ cm. Moore *et al.* (1982) have suggested such a model for behaviour observed in BL Lac itself during an intensive observing campaign in 1979. One possibility is that the subunits are emission knots in a relativistic jet. High polarized knots

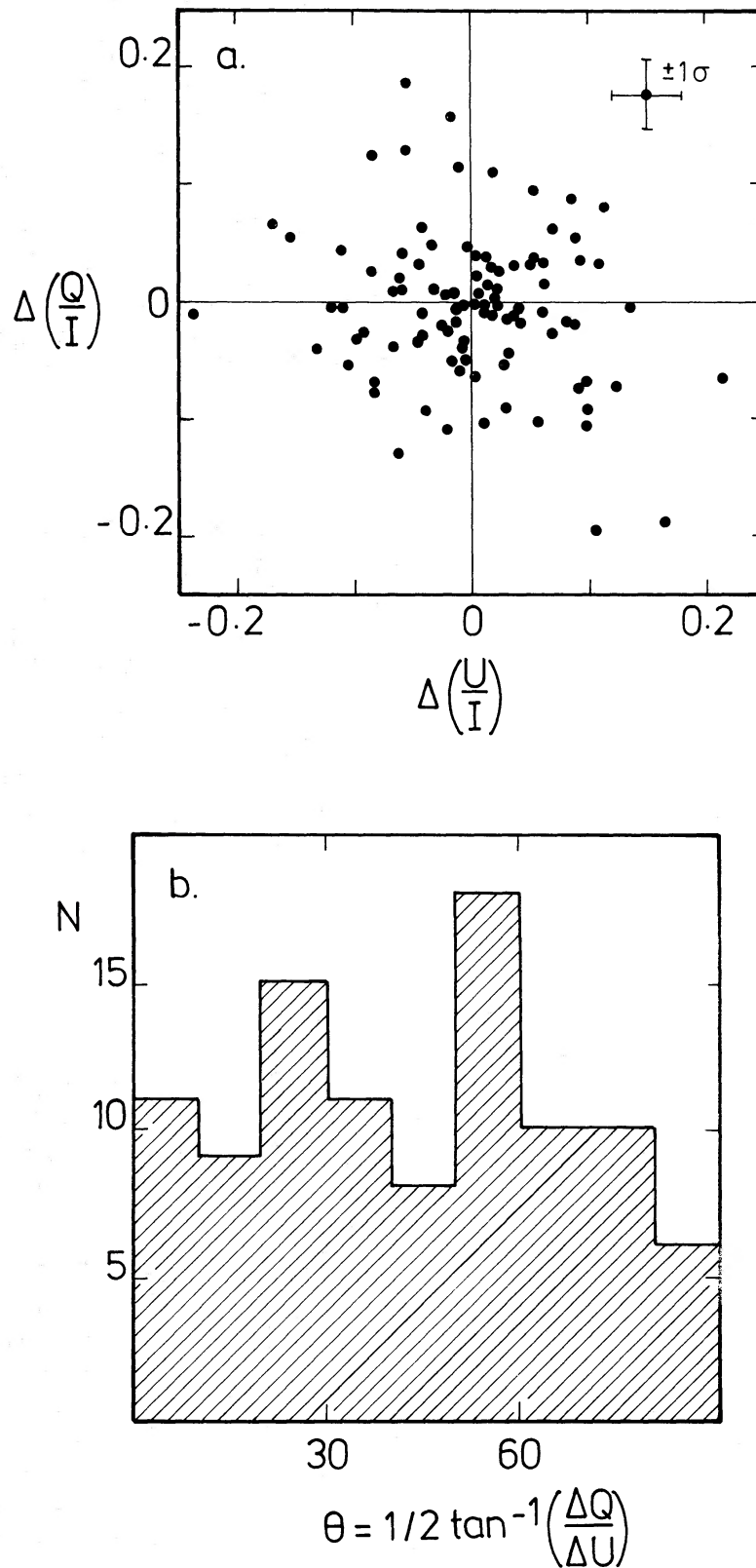


Figure 7. (a) Internight changes in $\Delta(Q/I)$ and $\Delta(U/I)$ are plotted. The uniform distribution of points around the origin indicates that the distribution of p_{Var} is unaffected by instrumental biases; (b) The distribution of angle $\theta = 1/2 \tan^{-1}(\Delta Q/\Delta U)$ is plotted.

have been resolved optically in the M87 jet (Sulentic, Arp & Lowe 1979) and they have been seen in *VLBI* maps of many radio sources (Miley 1980). The non-variable component might then correspond to the uniform volume emission of the jet, or alternatively, to an accretion disc surrounding the central power source. However, changes in polarization and flux appear totally uncorrelated for four of the objects, and there are many significant individual examples of large changes in polarization with little or no corresponding change in total flux. This has no interpretation in the multiple sub-unit model where the flux and polarization changes should always be correlated. It is also difficult to explain using the incoherent synchrotron model. Propagation and optical depth effects will be small at infrared wavelengths, so polarization should reflect the magnetic field geometry. Changes in Faraday optical depth cannot be responsible because they would be accompanied by large swings in position angle, which are not observed.

4.6 WAVELENGTH-DEPENDENT POLARIZATION

In Paper I, 0735 + 178 and 0235 + 164 were found to have wavelength-dependent polarization, with the polarization increasing towards shorter wavelengths. Further observations of 0735 + 178 have confirmed the existence of wavelength-dependent polarization, with variable slope. Bailey, Hough & Axon (1982) have recently found evidence for wavelength-dependent polarization where the amount of $p(\lambda)$ depends on the degree of polarization; their data having better polarimetric precision but poorer wavelength resolution and photometric precision than the data discussed here. This important result will be a key to the synchrotron modelling of BL Lac objects. The most likely explanation for strong $p(\lambda)$ behaviour involves the superposed spectral variations of physically separate emitting regions (Puschell *et al.* 1983; Impey, Brand & Tapia 1982b), so both polarimetric and photometric observations will be needed in future.

4.7 THE $Q-U$ PLANE

Another way of studying the variable polarization of BL Lac objects is a $Q-U$ diagram in which the normalized Stokes parameters Q/I and U/I are plotted on the x and y axes. In a $Q-U$ plot, contours of constant polarization are circles and contours of constant position angle are radii. The distance from a data point on the diagram to the origin is the polarization p , and the vector joining the two data points on successive nights represents p_{var} . Position angles on the sky are measured with respect to the Q axis. In Paper I, we observed that the polarization trajectories for monitoring runs on several objects seemed to follow characteristic paths of constant position angle and polarization. With a much improved database we can investigate this behaviour statistically. There are 97 vectors each representing a change in polarization between successive nights. There are no instrumental effects biasing the orientation of the p_{var} vectors, since the values of p_{var} are uniformly distributed around the origin of a plot of $\Delta(Q/I)$ vs. $\Delta(U/I)$ (Fig. 7). Therefore, the p_{var} vectors are uniformly distributed in angle on the $Q-U$ plane.

To confirm the effect found in Paper I, the coordinate system for measuring position angles must be transformed. Fig. 8 shows the two reference frames. In the normal (celestial) system, angles are measured between the vector p_{var} and the Q -axis. In the new system, angles are measured between the vector p_{var} and a radius drawn to connect the origin and \bar{p} (the midpoint of p_{var}). If this angle is labelled ϕ then $\phi=0^\circ$ represents a change in polarization at a constant position angle, and $\phi=90^\circ$ represents a change in position angle at a constant polarization. The distribution of ϕ is plotted in Fig. 9a and it is clearly non-uniform. There is a large peak near $\phi=90^\circ$, at the 3σ level.

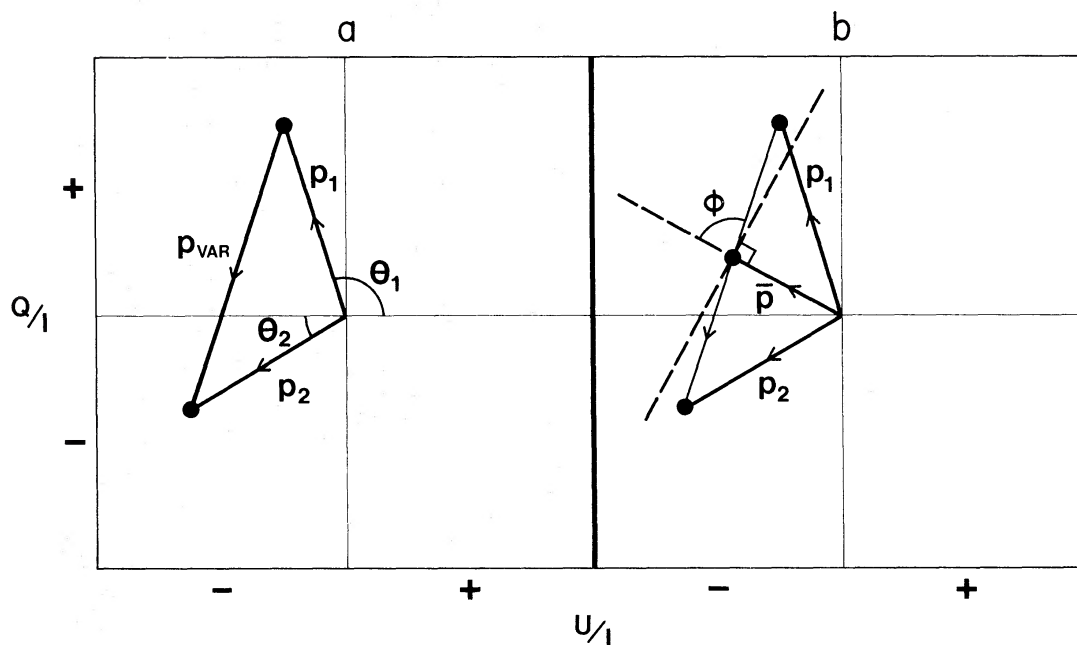


Figure 8. (a) Normalized Stokes parameters Q/I and U/I are plotted in the celestial system. The vectors p_1 and p_2 have degrees of polarization p_1 and p_2 and position angles θ_1 and θ_2 . The inter-night change in polarization is given by $p_{VAR} = p_2 - p_1$. (b) Q/I and U/I are plotted in a reference frame defining the angle ϕ , which is the angle measured between the vectors \bar{p} and p_{VAR} .

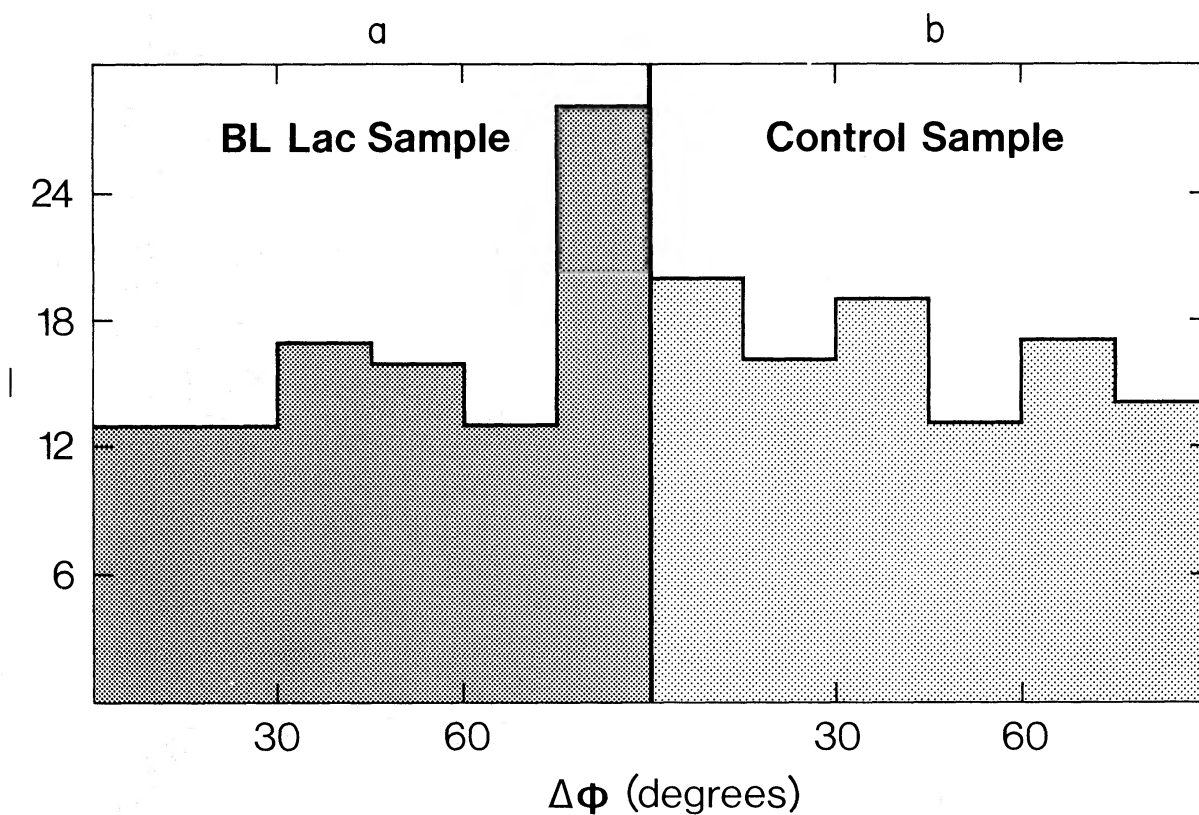


Figure 9. (a) The distribution of ϕ is plotted for 100 inter-night observations of polarization. The measurements involve the J , H and K band and include all objects in the sample; (b) This distribution of ϕ is plotted for a control sample of polarized, variable stars. The observations were made by K. Serkowski.

Since many of the individual measurements have poor signal-to-noise (in terms of ΔQ and ΔU), it is possible that the peak at 90° is an artifact of noisy data. Therefore, the same test was performed on a control sample of data: optical polarimetry of red variable stars by K. Serkowski (unpublished data). Many of the stars have long monitoring runs and the same number of data points were used. Although the physics of the polarization variations is completely different from BL Lac objects, the mean signal-to-noise of the two sets of measurements is similar. The Serkowski data is shown in Fig. 9b, and it is uniform in ϕ to well within the statistical errors.

The implication of the ϕ distribution is that position angle rotations and polarization changes are 'decoupled': rotations in position angle are not generally accompanied by polarization changes. There are physical reasons for preserving the distinction between p and ϕ . In a synchrotron model, changing p may be due to the addition of several variable components or to the compression of the magnetic field in a high surface brightness region. Changing ϕ may be due to rotating field lines or to the addition of several components; therefore, separate mechanisms may be at work when p and ϕ vary.

5 Conclusions

The important characteristics of individual BL Lac objects are summarized in Table 4 by a check against the corresponding property. Column (2) indicates a thermal component from the two-colour plot, and column (3) indicates an estimated $1-10 \mu\text{m}$ luminosity near or above the Eddington limit. Columns (4) and (5) show the presence of wavelength-dependent polarization and rapid position angle rotations (> 20 per cent/day). Column (6) indicates whether the internight changes in total and polarized flux are correlated or uncorrelated.

There has been much theoretical interest recently in relativistic jets as the source of con-

Table 4. Checklist of properties of BL Lac objects.

(1)	(2)	(3)	(4)	(5)	(6)
Object	Thermal component	$L_{\text{MAX}} \gtrsim L_{\text{Edd}}$	$p(\lambda)$	$\theta(t)$	$\Delta p \propto \Delta I$
0235+164	—	✓	✓	✓	x
0735+178	—	—	✓	✓	✓
0754+101	—	—	—	—	—
0851+202	—	—	—	✓	✓
1156+295	—	✓	—	✓	x
1308+326	—	✓	—	—	x
1418+546	—	—	—	✓	—
1641+399	—	✓	—	—	x
1652+398	✓	—	—	—	—
1727+503	✓	—	—	—	—
2155-304	✓	—	—	—	—
2223-052	—	✓	—	—	—

tinuum energy in many types of radio sources (Blandford 1981). There have also been ambitious attempts to link many types of active nuclei in terms of a relativistic jet seen at different angles to the observer's line-of-sight (Marscher 1980, Blandford & Königl 1979, Königl 1981, Blandford & Rees 1978, Scheuer & Readhead 1979). These models try to account for the differences in radio, optical, and X-ray properties between radio-quiet quasars, radio-loud quasars, low frequency radio variables, OVV quasars, and BL Lac objects. Geometry plays an important role in these scenarios, and in all cases BL Lac objects are thought to be sources with the smallest viewing angle to the jet axis. Unfortunately, the evidence for this unified picture is mostly circumstantial, since most of the VLBI maps of jets have been of low luminosity sources, and it is a large jump to apply these structures to high luminosity quasars and BL Lac objects. However, recent theoretical work has shown that polarization data can be a powerful discriminant between various types of relativistic jet (Bjornsson 1982). These polarization observations offer a good change to test jet models by comparing luminosity and polarization properties of the data with the expected viewing angle and magnetic field geometry of the jet.

Acknowledgments

We thank the panel for the allocation of telescope time, and Terry Lee and the UKIRT staff for excellent support. In particular, John Clark and Malcolm Stewart contributed greatly to the implementation of the hardware and software for the polarimeter. We are grateful to Bill Zealey for able assistance at the telescope. We also thank the referee for suggestions which considerably improved the clarity of this paper. CDI acknowledges the receipt of an SERC/NATO Fellowship, and part of the work was carried out while in receipt of an SERC Studentship.

References

- Aller, H. D., Aller, M. F. & Hodge, P. E., 1981. *Astr. J.*, **86**, 325.
- Angel, J. R. P., Boroson, T. A., Adams, M. T., Duerr, R. E., Giampapa, M. S., Gresham, M. S., Gural, P. S., Hubbard, E. N., Kopriva, D. A., Moore, R. L., Peterson, B. M., Schmidt, G. D., Turnshek, D. A., Wilkerson, M. S. & Zotov, N. V. 1978. *Pittsburgh Conference on BL Lac Objects*, p. 117, ed. Wolfe, A. M., University of Pittsburgh.
- Angel, J. R. P. & Stockman, H. S., 1980. *Ann. Rev. Astr. Astrophys.*, **18**, 321.
- Bailey, J., Hough, J. H. & Axon, D. J., 1984. *Mon. Not. R. astr. Soc.*, **203**, 339.
- Becker, W., 1937. *Z. für Astrophys.*, **15**, 225.
- Beichman, C. A., Prardo, S. H., Neugebauer, G., Soifer, B. T., Matthews, K. & Wooten, H. A., 1981. *Astrophys. J.*, **247**, 780.
- Bjornsson, C.-I., 1982. *Astrophys. J.*, **260**, 855.
- Blandford, R. D. & Rees, M. J., 1978. *Pittsburgh Conference on BL Lac Objects*, p. 328. ed Wolfe, A. M., University of Pittsburgh.
- Blandford, R. D. & Königl, A., 1979. *Astrophys. J.*, **232**, 34.
- Blandford, R. D. *XXIII COSPAR Conference*, Budapest 1981, Reidel, Dordrecht, Holland, in press.
- Bonoli, F., Braccisi, L., Frederici, L., Zitelli, V. & Formiggini, L., 1979. *Astr. Astrophys. Suppl.*, **35**, 391.
- Borra, E. F., 1983. *Astrophys. J.*, **273**, L55.
- Chanan, G. A., Margon, B., Helfand, D. J., Downes, R. A. & Chance, D., 1981. *Bull. Am. Astr. Soc.*, **13**, 848.
- Condon, J. J., Hicks, P. D. & Jauncey, D. L., 1977. *Astr. J.*, **82**, 692.
- Conway, R. G., Haves, P., Kronberg, P. P., Stannard, C., Vallee, J. P. & Wardle, J. F. C., 1974. *Mon. Not. R. astr. Soc.*, **168**, 137.
- Cotton, W. D., Counselman, C. C., Geller, R. B., Shapiro, I. I., Wittels, J. J., Hinteregger, H. F., Knight, C. A., Rogers, A. E. E., Whitney, A. R. & Clark, T. A., 1979. *Astrophys. J.*, **229**, L115.

- Craine, E. R., Duerr, R. & Tapia, S., 1978. *Pittsburgh Conference on BL Lac Objects*, p. 99, ed Wolfe, A. M., University of Pittsburgh.
- Eachus, L. J. & Liller, W., 1975. *Astrophys. J.* **200**, L61.
- Elliott, J. L. & Shapiro, S. L., 1974. *Astrophys. J.*, **192**, L3.
- Elvius, A., 1968. *Lowell Obs. Bull.*, **142**, 75.
- Epstein, E. E., Fogarty, W. G., Mottmann, J. & Schneider, E., 1982. *Astr. J.*, **87**, 44.
- Frogel, J. A., Persson, S. E., Aaronson, M. A. & Matthews, K., 1978. *Astrophys. J.*, **220**, 75.
- Glassgold, A. E., Bregman, J. N., Huggins, P. J., Kinney, A. L., Pica, A. J., Pollock, J. T., Leacock, R. J., Smith, A. G., Webb, J. R., Wiśniewski, W. Z., Jeske, N., Spinrad, H., Henry, R. B. C., Miller, J. S., Impey, C., Neugebauer, G., Aller, M. F., Aller, H. D., Hodge, P. E., Balonek, T. J., Dent, W. A. & O'Dea, C. P., 1983. *Astrophys. J.*, **274**, 101.
- Hawkins, M. R. S., 1983. Proc. *Quasars and Gravitational Lenses*, 24th Liege Astrophysical Symposium, p. 36, Université de Liège.
- Impey, C. D. & Brand, P. W. J. L., 1981. *Nature*, **292**, 814.
- Impey, C. D. & Brand, P. W. J. L., 1982. *Mon. Not. R. astr. Soc.*, **200**, 19.
- Impey, C. D., Brand, P. W. J. L., Wolstencroft, R. D. & Williams, P. M., 1982a. *Mon. Not. R. astr. Soc.*, **200**, 19 (Paper I).
- Impey, C. D., Brand, P. J. W. L. & Tapia, S. 1982b. *Mon. Not. R. astr. Soc.*, **198**, 1.
- Kellerman, K. I., Jauncey, D. L., Cohen, M. H., Shaffer, B. B., Clark, B. G., Broderick, J., Ronnang, B., Rydbeck, O. E. H., Matreyenko, L., Moiseyev, I., Vitkevitch, V. V., Cooper, B. F. C. & Batchelor, R., 1971. *Astrophys. J.*, **179**, 1.
- Kinman, T. D., 1976. *Astrophys. J.*, **205**, 1.
- Knacke, R. F., Capps, R. W. & Johns, M., 1976. *Astrophys. J.*, **210**, L69.
- Konigl, A., 1981. *Astrophys. J.*, **243**, 700.
- MacLeod, J. M. & Andrew, B. H., 1968. *Astrophys. Lett.*, **1**, 243.
- Marscher, A. P., 1980. *Astrophys. J.*, **235**, 386.
- Miley, G., 1980. *Ann. Rev. Astro. Astrophys.*, **18**, 165.
- Miller, J. S., 1978. *Comm. Astrophys.*, **7**, 175.
- Miller, J. S. & Hawley, S. A., 1977. *Astrophys. J.*, **212**, L47.
- Miller, J. S., French, H. B. & Hawley, S. A., 1978. *Astrophys. J.*, **219**, L85.
- Moore, R. L. & Stockman, H. S., 1981. *Astrophys. J.*, **243**, 6.
- Moore, R. L., McGraw, J., Angel, J. R. P., Duerr, R., Lebofsky, M., Rieke, G., Wisniewski, M., Axon, D., Bailey, J., Hough, J., Thompson, I., Breger, M., Schulz, H., Clayton, J., Martin, P., Miller, J., Schmidt, G., Africano, J. & Miller, H., 1982. *Astrophys. J.*, **260**, 415.
- Neugebauer, G., Oke, J. B., Becklin, E. E. & Matthews, K., 1979. *Astrophys. J.*, **230**, 79.
- O'Dell, S. L., Puschell, J. J., Stein, W. A. & Warner, J. W., 1978. *Astrophys. J. Suppl.*, **38**, 267.
- Puschell, J. J. & Stein, W. A., 1980. *Astrophys. J.*, **237**, 331.
- Puschell, J. J., Jones, T. W., Phillips, A. C., Rudnick, L., Simpson, E., Sitko, M., Stein, W. A. & Moneti, A., 1983. *Astrophys. J.*, **265**, 625.
- Puschell, J. J., Stein, W. A., Jones, T. W., Warner, J. W., Owen, F., Rudnick, L., Aller, H. & Hodge, P., 1979. *Astrophys. J.*, **227**, L11.
- Rieke, G. H. & Kinman, T. D., 1974. *Astrophys. J.*, **192**, L115.
- Rieke, G. H., Grasdalen, G. L., Kinman, T. D., Hintzen, P., Wills, B. J. & Wills, D., 1976. *Nature*, **260**, 754.
- Rieke, G. H., Lebofsky, M. J., Kemp, J. C., Coyne, G. V. & Tapia, S., 1977. *Astrophys. J.*, **218**, L37.
- Rieke, G. H. & Lebofsky, M. J., 1979. *Ann. Rev. Astr. Astrophys.*, **17**, 477.
- Rudnick, L., Owen, F. N., Jones, T. W., Puschell, J. J. & Stein, W. A., 1978. *Astrophys. J.*, **225**, L5.
- Scheuer, P. A. G. & Readhead, A. S. C., 1979. *Nature*, **277**, 182.
- Schmidt, M., 1974. *Astrophys. J.*, **193**, 505.
- Schmitt, J. L., 1968. *Nature*, **218**, 663.
- Seielstad, G. A., Cohen, M. H., Linfield, R. P., Moffett, A. T., Rommey, J. D. & Schitizzi, R. T., 1979. *Astrophys. J.*, **229**, 53.
- Snyder, W. A., Davidson, A., Wood, K., Kinzer, R., Smathers, H., Shulman, S., Meekins, J., Yentis, D., Evans, W., Bryan, E., Chubb, T., Freidman, H., & Margon, B. 1980. *Astrophys. J.*, **237**, L11.
- Stein, W. A., O'Dell, S. L. & Strittmatter, P. A., 1976. *Ann. Rev. Astr. Astrophys.*, **14**, 173.
- Stocke, J., Liebert, J., Stockman, H., Danziger, J., Lub, J., Maccararro, T., Griffiths, R., & Giommi, P. 1982. *Mon. Not. R. astr. Soc.*, **200**, 27P.
- Stockman, H. S. & Angel, J. R. P., 1978. *Astrophys. J.*, **220**, L67.
- Sulentic, J. W., Arp, H. & Lorre, J., 1979. *Astrophys. J.*, **233**, 44.

- Tananbaum, H., Avni, Y., Branduard, G., Elvis, M., Fabbiano, G., Feigelson, E., Giacconi, R., Henry, J. P., Pye, J. P., Soltan, A. & Zamorani, G., 1980. *Astrophys. J.*, **234**, L9.
- Tapia, S., Craine, E. R., Gearhart, M. R., Pacht, E. & Kraus, J., 1977. *Astrophys. J.*, **215** L71.
- Usher, P. D., 1975. *Astrophys. J.*, **198**, L57.
- Veron, P., 1978. In *Pittsburgh Conference on BL Lac Objects*, p. 20, ed Wolfe, A. M., University of Pittsburgh.
- Visvanathan, N., 1973. *Astrophys. J.*, **179**, 1.
- Wade, R., 1980. PhD dissertation, California Institute of Technology, California.
- Weiler, K. W. & Johnston, K. J., 1980. *Mon. Not. R. astr. Soc.*, **190**, 269.
- Wills, D., Wills, B. J., Breger, M. & Hsu, J. C., 1980. *Astr. J.*, **85**, 1555.